better than 0.3 K. At 100 K, cell constants were obtained from a least-squares fit of the setting angles of 25 reflections. A summary of crystal and intensity collection data is given in Table III. A total of 6626 reflections were recorded in two shells (1–20° and 20–25°) by procedures described elsewhere.[18] At the end of the second shell data collection, the crystal broke down and no attempt to collect the few missing reflections was made with a new crystal. Intensity standards, recorded periodically, showed only random, statistical fluctuations. Data reduction was then performed,[19] and empirical absorption corrections[20] were made (μ = 11.9 cm^{-1}; calculated transmission range 0.95–1.00), psi scan having been made before registration of the data. A total of 4994 reflections with $I > 3\sigma(I)$ were considered as observed and used for structure resolution.

Structure Solution and Refinement. The structure was solved[21] by the heavy-atom method. Successive difference Fourier maps and least-squares refinement cycles revealed the positions of all non-hydrogen atoms.

All non-hydrogen atoms were refined anisotropically, except phenyl rings which were refined as isotropic rigid groups (C–C = 1.395 Å). Hydrogen atoms were all located on a difference Fourier map and were included in calculations in constrained geometry (C–H = 0.97 Å) with fixed isotropic temperature factors, except for that bonded to C(12) which was allowed to vary.

The atomic scattering factors used were those proposed by Cromer and Waber[22] with anomalous dispersion effects.[23] Scattering factors for the hydrogen atoms were taken from Stewart et al.[24]

The final full-matrix least-squares refirement converged to $R = \sum||F_o| - |F_c||/\sum|F_o| = 0.019$ and $R_W = [\sum(|F_o| - |F_c|)^2/\sum w|F_o|^2]^{1/2} = 0.020$ with $w = 1/\sigma^2(F_o)$. The error in an observation of unit weight was $S = [\sum w(|F_o| - |Fc|)^2/(n - m)]^{1/2} = 1.0$ with $n = 4994$ observations and $m = 332$ variables. An analysis of variance showed no unusual trends. In the last cycle of refinement the shifts for all parameters but those for H(C12) were less than 0.05σ. A final difference Fourier showed a residual electron density of 0.3 e/Å^3. The final fractional atomic coordinates are listed in Table IV.

Registry No. $Fe_3(CO)_9(\mu_3\text{-}COC_2H_5)(\mu_3\text{-}CCH_2Ph)$, 110698-07-2; $Fe_3(CO)_9(\mu_3\text{-}COC_2H_5)(\mu_3\text{-}C(CH_2)_3CH_3)$, 110698-08-3; $Fe_3(CO)_9(\mu_3\text{-}COC_2H_5)(\mu_3\text{-}CCH_2C(O)CH_3)$, 110698-09-4; $Fe(CO)_9(\mu_3\text{-}COC_2H_5)(\mu_3\text{-}CCH_2C(O)OCH_3)$, 110698-10-7; $[PPh_4][Fe_3(CO)_{10}(\mu_3\text{-}CCH_2Ph)]$, 109993-92-2; $[PPh_4][Fe_3(CO)_{10}(\mu_3\text{-}C(CH_2)_3CH_3)]$, 109993-94-4; $[PPh_4][Fe_3(CO)_{10}(\mu_3\text{-}CCH_2C(O)CH_3)]$, 109993-84-2; $[PPh_4][Fe_3(CO)_{10}(\mu_3\text{-}CCH_2C(O)OCH_3)]$, 109993-96-6; $[PPh_4][Mn(CO)_5]$, 67047-43-2; $[PPh_4][Fe_3(CO)_9(\mu_3\text{-}\eta^2\text{-}CCCH_2Ph)]$, 110698-12-9; $[PPh_4][Fe_3(CO)_9(\mu_3\text{-}\eta^2\text{-}CC(CH_2)_3CH_3)]$, 110698-14-1; $[PPh_4][Fe_3(CO)_9(\mu_3\text{-}\eta^3\text{-}C(OC_2H_5)CCHC(O)CH_3)]$, 110698-16-3; $[PPh_4][Fe_3(CO)_9(\mu_3\text{-}\eta^3\text{-}C(OC_2H_5)CHC(O)OCH_3)]$, 110698-18-5; $[PPh_4]_2[Fe_3(CO)_{11}]$, 95765-17-6; $[PPh_4][Fe_3(CO)_9(CCH)]$, 110698-20-9; $[PPh_4][Fe_3(CO)_9(\mu_3\text{-}\eta^2\text{-}CCCH_2C(O)CH_3)]$, 110698-22-1; $[PPh_4][Fe_3(CO)_9(\mu_3\text{-}\eta^2\text{-}CCCH_2C(O)OCH_3)]$, 110698-24-3; $Mn_2(CO)_{10}$, 10170-69-1; $HFe_3(CO)_9(\mu_3\text{-}CCH)$, 83802-15-7; Fe, 7439-89-6; ethoxyacetylene, 927-80-0.

Supplementary Material Available: Tables of atomic coordinates, hydrogen and thermal parameters, and bond lengths and angles (6 pages); a table of structure factors (24 pages). Ordering information is given on any current masthead page.

(18) Mosset, A.; Bonnet, J.-J.; Galy, J. *Acta Crystallogr., Sect. B: Struct. Crystallogr. Cryst. Chem.* **1977**, *B33*, 2639–2644.
(19) Frentz, B. A. *SDP, Structure Determination Package*; Enraf-Nonius: Delft, Holland 1982.
(20) North, A. C. T.; Phillips, D. C.; Mathews, F. S. *Acta Crystallogr., Sect. A: Cryst. Phys., Diffr., Theor. Gen. Crystallogr.* **1968**, *A24*, 351–359.
(21) Sheldrick, G. M. *SHELX76, Program for Crystal Structure Determination*; University of Cambridge: Cambridge, England, 1976.
(22) Cromer, D. T.; Waber, J. T. *International Tables for X-Ray Crystallography*; Ibers, J. A., Hamilton, W. C., Eds.; Kynoch: Birmingham, England, 1974; Vol. IV, Table 2.2.B., pp 99–101.
(23) Cromer, D. T., ref 21, Table 2.3.1., p 149.
(24) Stewart, R. F.; Davidson, E. R.; Simpson, W. T. *J. Chem. Phys.* **1965**, *42*, 3175–3187.

Molecular Orbital Analysis of Dicarbido–Transition-Metal Cluster Compounds

Jean-François Halet† and D. Michael P. Mingos*

Inorganic Chemistry Laboratory, University of Oxford, South Parks Road, Oxford OX1 3QR, United Kingdom

Received April 7, 1987

Molecular orbital calculations on dicarbido–transition-metal carbonyl cluster compounds have shown that the bonding between C_2 and the metal cage results primarily from electron donation from the C_2 σ_p- and π-bonding molecular orbitals and back donation from filled metallic molecular orbitals to the C_2 π^* orbitals. The bonding therefore follows closely the Chatt–Dewar–Ducanson model that has been established previously for ethyne and ethene complexes but not for interstitial moieties. The C–C separation in the dicarbido clusters depends critically on the geometric constraints imposed by the metal cage and the extent of forward and back donation. In these clusters where the carbon atoms are in adjacent trigonal-prismatic sites the calculated formal bond order is between 1.0 and 1.5, which agrees well with the observed C–C bond lengths.

Introduction

Carbido–transition-metal carbonyl clusters have been studied in some detail from both an experimental[1] and a theoretical[2] point of view because they are thought to be good models for intermediates in heterogeneous Fischer–Tropsch catalytic processes. The study of polycarbido compounds have received much less attention although examples of such compounds have been recognized in both cluster chemistry and solid-state chemistry. In solid-state chemistry the bonded carbon–carbon unit was characterized initially in the simple binary compounds[3] like CaC_2,

†Permanent address: Laboratoire de Cristallochimie, U.A. 254, University of Rennes, Rennes, France.

(1) For a review see: (a) Tachikawa, M.; Muetterties, E. L. *Prog. Inorg. Chem.* **1981**, *28*, 203. (b) Bradley, J. S. *Adv. Organomet. Chem.* **1983**, *22*, 1. (c) Vargas, M. D.; Nicholls, J. N. *Adv. Inorg. Chem. RadioChem.* **1986**, *30*, 123.
(2) See, for example: (a) Wijeyesekara, S. D.; Hoffmann, R. *Organometallics* **1984**, *3*, 949. (b) Wijeyesekara, S. D.; Hoffmann, R.; Wilker, C. N. *Organometallics* **1984**, *3*, 962. (c) Halet, J.-F.; Saillard, J.-Y.; Lissillour, R.; McGlinchey, M. J.; Jaouen, J. *Organometallics* **1986**, *5*, 139. (d) Brint, P.; O'Cuil, K.; Spalding, T. R. *Polyhedron* **1986**, *5*, 1791.

0276-7333/88/2307-0051$01.50/0

Table I. Characterized Polycarbido-Transition-Metal Clusters

cluster compd	carbon cage[a]	d_{C-C}, Å	VEC[b]	Δ_i[c]	ref
$Co_6(CO)_{14}S(C_2)$			94	22	8
$[Co_6Ni_2(CO)_{16}(C_2)]^{2-}$	tp	1.494	116	20	9
$[CO_3Ni_7(CO)_{15}(C_2)]^{3-}$	ctp	1.430	138	18	10
$[Co_3Ni_7(CO)_{16}(C_2)]^{2-}$	ctp	1.480	139	19	11
$[Ni_{10}(CO)_{16}(C_2)]^{2-}$	ctp	1.405	142	22	12
$[Ru_{10}(CO)_{24}(C)_2]^{2-}$	o	2.984	138	18	13
$[Co_{11}(CO)_{22}(C_2)]^{3-}$	tp–sa	1.62/1.66	154	22	14
$[Rh_{12}(CO)_{23}(C)_2]^{3-}$	tp	3.20/3.32	165	21	15
$[Rh_{12}(CO)_{23}(C)_2]^{4-}$	tp	3.371	166	22	16
$[Rh_{12}(CO)_{24}(C)_2]^{2-}$	tp	3.30	166	22	17
$Rh_{12}(CO)_{25}(C_2)$	tp–sa	1.480	166	22	18
$[Rh_{12}H(CO)_{23}(N)_2]^{3-}$	tp–sa	2.92	168	24	19
$[Co_{13}(CO)_{24}(C)_2]^{3-}$	tp–ctp	2.554	176	20	20
$[Co_{13}(CO)_{23}(C)_2]^{4-}$	ctp	2.986	177	21	21
$[Rh_{15}(CO)_{28}(C)_2]^{-}$	o		200	20	22
$[Ni_{16}(CO)_{23}(C_2)_2]^{4-}$	$t\nu_2o$	1.38/2.88	226	34	23
$[Ni_{34}H(CO)_{38}(C)_4]^{5-}$	tp		438		24
$[Ni_{35}(CO)_{39}(C)_4]^{6-}$	tp		450		24
$[Ni_{38}H(CO)_{42}(C)_6]^{5-}$	sa	3.25/3.32	494		25

[a] Abbreviations: tp, trigonal prism; ctp, capped trigonal prism; o, octahedron; sa, square-antiprism; $t\nu_2o$, truncated ν_2 octahedron. [b] Valence electron count. [c] Skeletal electron number.

MC_2 (M = Th, U, Lu, Tb, La), La_2C_3, and more recently $Gd_2Cl_2C_2$.[4] In CaC_2 and ThC_2 the C_2 fragment lies at the center of an octahedron of metal atoms, and in La_2C_3 it lies at the center of a Δ-dodecahedron of metal atoms. In these compounds an ionic view of the bonding in conjunction with a qualitative molecular orbital scheme for the dimeric C_2 unit is sufficient to account for the majority of the observed variation in C–C bond lengths,[5] i.e. $Ca^{2+}C_2^{2-}$ (1.191 Å) or $M^{3+}C_2^{3-}$ (1.276–1.315 Å). In $Gd_2Cl_2C_2$ the C_2 units occupy the octahedral holes of two adjacent close-packed planes of Gd atoms. The observed C–C distance of 1.36 Å is rationalized by an effective charge of 4– to C_2. In contrast in the clusters $Gd_{10}C_4Cl_{18}$ the C–C bond length is 1.47 Å, consistent with the presence of C_2^{6-} units in octahedral holes.[6] Although in La_2C_3 the C_2 dimer is assigned a formal charge of 4–, the bond length is very short (1.236 Å), suggesting that some of the electrons occupy a metallic conduction band.

Examples of polycarbido cluster compounds with up to 38 metal atoms have been characterized.[7] Table I summarizes the relevant structural data for polycarbido–metal carbonyl cluster compounds. In the majority of compounds the carbon atoms are not linked by a direct C–C bond, but there are some interesting examples of ethanido cluster compounds with C–C bond lengths lying between 1.37 and 1.66 Å. All the ethanido cluster compounds have been observed for the cobalt and nickel triads, and the carbon atoms lie at the centers of a pair of polyhedra sharing a square face. The individual carbon atoms lie at the centers of trigonal-prismatic, capped trigonal-prismatic, or square-antiprismatic metal polyhedra.

The occurrence of ethanido– rather than dicarbido–metal carbonyl clusters (with well-separated carbon atoms) is dependent on several factors and is not a simple function of the total number of valence electrons. For example $Rh_{12}(CO)_{25}(C_2)$ and $[Rh_{12}(CO)_{24}(C_2)]^{2-}$ are isoelectronic, but the former has the carbon atoms occupying sites at the centers of face-sharing trigonal-prismatic and square-antiprismatic metal cluster (C–C = 1.48 Å) and the latter has the carbon atoms occupying the centers of a pair of distorted face-sharing square antiprisms (C–C = 3.30 Å).

In contrast to the situation encountered in solid-state chemistry the C–C bond is not necessarily lengthened by addition of valence electrons to the cluster. For example, in both $[Ni_{10}(CO)_{16}(C_2)]^{2-}$ and $[Co_3Ni_7(CO)_{15}(C_2)]^{3-}$ the C–C bond lengths are nearly identical, 1.405 and 1.430 Å, respectively, although the former compound has four additional valence electrons (see Table I).

This paper utilizes extended Hückel molecular orbital calculations to interpret the following interesting features associated with ethanido and related X–X encapsulated cluster compounds. What is the nature of the bonding between the C–C unit, or more generally an X–X fragment, and the skeletal molecular orbitals of surrounding carbonyl cluster? How is this bonding influenced by the addition or loss of electrons? What are the primary factors influencing the total number of skeletal electron pairs associated with these cluster compounds?

As a prelude to a discussion of these important electronic factors, it is instructive to consider the purely geometric factors associated with encapsulating an X–X fragment in a pair of polyhedra sharing a common face.

Geometric Considerations

Table II summarizes the calculated X–X and X–M distances for pairs of polyhedra with the X atoms located at the centroids of the polyhedra. These idealized calculations are illustrated for metal–metal distances of 2.54 and

(3) (a) Atoji, M. *J. Chem. Phys.* **1961**, *35*, 1950. (b) Atoji, M.; Williams, D. E. *J. Chem. Phys.* **1961**, *35*, 1960. (c) Bowman, A. L.; Krikorian, N. H.; Arnold, G. P.; Wallace, T. C. *Acta Crystallogr. Sect. B: Struct. Crystallogr. Cryst. Chem.* **1968**, *B24*, 1121.
(4) Schwarz, C.; Simon, A., quoted in ref 5b.
(5) (a) Burdett, J. K.; McLarnan, T. J. *Inorg. Chem.* **1982**, *21*, 1119. (b) Miller, G. J.; Burdett, J. K.; Schwarz, C.; Simon, A. *Inorg. Chem.* **1986**, *25*, 4437.
(6) Warkentin, E.; Masse, R.; Simon, A. *Z. Anorg. Allg. Chem.* **1982**, *491*, 323. For a theoretical study see Satpathy, S.; Andersen, O. *Inorg. Chem.* **1985**, *24*, 2604.
(7) Longoni, G.; Ceriotti, A.; Marchionna, M.; Piro, G., to be submitted for publication.
(8) Stanghellini, P. L. *XVI Cong. Naz. Chim. Inorg.*, Ferrara, 1983, 406. Gervasio, G.; Rossetti, R.; Stanghellini, P. L.; Bor, G. *Inorg. Chem.* **1984**, *23*, 2073.
(9) Arrigoni, A.; Ceriotti, A.; Della Pergola, R.; Manassero, M.; Masciocchi, N.; Sansoni, M. *Angew. Chem., Int. Ed. Engl.* **1984**, *23*, 322.
(10) Longoni, G.; Ceriotti, A.; Della Pergola, R.; Manassero, M.; Perego, M.; Piro, G.; Sansoni, M. *Philos. Trans. R. Soc. London, Ser. A* **1982**, *No. 308*, 47.
(11) Arrigoni, A.; Ceriotti, A.; Della Pergola, R.; Longoni, G.; Manassero, M.; Sansoni, M. *J. Organomet. Chem.* **1985**, *296*, 243. Manassero, M., personal communication.
(12) Ceriotti, A.; Longoni, G.; Manassero, M.; Masciocchi, N.; Resconi, L.; Sansoni, M. *J. Chem. Soc., Chem. Commun.* **1985**, 181.
(13) Hayward, C.-M. T.; Shapley, J. R.; Churchill, M. R.; Bueno, C.; Rheingold, A. L. *J. Am. Chem. Soc.* **1982**, *104*, 7347.
(14) Albano, V. G.; Braga, D.; Ciani, G.; Martinengo, S. *J. Organomet. Chem.* **1981**, *213*, 293.
(15) Strumolo, D.; Seregni, C.; Martinengo, S.; Albano, V. G.; Braga, D. *J. Organomet. Chem.* **1983**, *252*, C93.
(16) Albano, V. G.; Braga, D.; Strumolo, D.; Seregni, C.; Martinengo, S. *J. Chem. Soc., Dalton Trans.* **1985**, 1309.
(17) Albano, V. G.; Braga, D.; Chini, P.; Strumolo, D.; Martinengo, S. *J. Chem. Soc., Dalton Trans.* **1983**, 249.
(18) Albano, V. G.; Chini, P.; Martinengo, S.; Sansoni, M.; Strumulo, D. *J. Chem. Soc., Dalton Trans.* **1978**, 459.
(19) Martinengo, S.; Ciani, G.; Sironi, A. *J. Chem. Soc., Chem. Commun.* **1986**, 1742.
(20) Albano, V. G.; Braga, D.; Fumagalli, A.; Martinengo, S. *J. Chem. Soc., Dalton Trans.* **1985**, 1137.
(21) Algano, V. G.; Braga, D.; Chini, P.; Ciani, G.; Martinengo, S. *J. Chem. Soc., Dalton Trans.* **1982**, 645.
(22) Albano, V. G.; Sansoni, M.; Chini, P.; Martinengo, S.; Strumolo, D. *J. Chem. Soc., Dalton Trans.* **1976**, 970.
(23) Ceriotti, A.; Longoni, G.; Piro, G.; Resconi, L.; Manassero, M.; Masciocchi, N.; Sansoni, M. *J. Chem. Soc., Chem. Commun.* **1985**, 1402.
(24) Ceriotti, A.; Fait, A.; Longoni, G.; Piro, G.; Resconi, L.; Demartin, F.; Manassero, M.; Masciocchi, N.; Sansoni, M. *J. Am. Chem. Soc.* **1986**, *108*, 5370.
(25) Ceriotti, A.; Fait, A.; Longoni, G.; Piro, G.; Demartin, F.; Manassero, M.; Masciocchi, N.; Sansoni, M. *J. Am. Chem. Soc.* **1986**, *108*, 8091.

Table II. Geometric Requirements for X_2 Dimers in Condensed Clusters as a Function of the Metal-Metal Separation (d (Å))

condensed polyhedra	X-X dist	X-M dist	d = 2.54 (Co) X-X	d = 2.54 (Co) X-M	d = 2.80 (Rh) X-X	d = 2.80 (Rh) X-M	suggested X_2 examples
octahedron–octahedron	0.817d	0.707d	2.08	1.8	2.29	1.98	
trigonal prism–trigonal prism	0.577d	0.764d	1.47	1.94	1.62	2.14	(C_2),[a] N_2
trigonal prism–square antiprism	0.709d	0.764d	1.8	1.94	1.99	2.14	(C_2),[a] $(N)_2$,[a] B_2, BN
		0.823d		2.09		2.3	
square antiprism–square antiprism	0.841d	0.823d	2.14	2.09	2.36	2.3	$(C)_2$,[a] Si_2
square antiprism–cube	0.921d	0.823d	2.34	2.09	2.58	2.3	Ge_2, As_2
		0.866d		2.20		2.43	
cube–cube	d	0.866d	2.54	2.20	2.80	2.43	Te_2

[a] Observed (see Table I).

2.80 Å, which are representative of typical Co–Co and Rh–Rh bond lengths in metal carbonyl clusters. The preference for the location of ethanido C_2 fragments in the cavities generated from a pair of trigonal prisms sharing a square face and a trigonal prism and a square antiprism arises primarily from geometric constraints. The separation of the polyhedral centroids leads to short C–C contacts (1.47–1.99 Å) and acceptable metal–carbon bond lengths (1.94–2.14 Å). In contrast the distance separating the centroids of a pair of square antiprisms is much longer than that requires for significant C–C bonding interactions (2.14–2.36 Å). The idealized C–C distance becomes even longer for a pair of cubes sharing a face. There are numerous examples of octahedral carbido clusters,[1] e.g. $Ru_6(CO)_{17}C$, but the condensation of a pair of octahedra through a triangular face does not provide a satisfactory basis of generating ethanido clusters because the centroids would be separated by 2.08–2.29 Å.

Although the condensation of trigonal prisms represents the most attractive geometric possibility for generating ethanido clusters, an alternative strategy can be based on encapsulating a C_2 moiety within a more spherical metal cluster. For example, a C–C bond length of 1.47 Å leads to satisfactory metal–carbon bond lengths (1.82 Å for M_{basal}–C, 2.13 Å for M_{apical}–C) if the C_2 moiety is incorporated in the center of a bicapped square antiprism with metal–metal bond lengths of 2.54 Å. The geometric considerations stated above have suggested that the most suitable ethanido cluster geometries are those based on a bicapped square antiprism and a pair of trigonal prisms sharing a square face. Therefore the subsequent section concentrates on extended Hückel molecular orbital calculations on such systems.

Although no transition-metal cluster compounds with other X–X entities have been characterized, there are many examples in solid-state chemistry of for instance dichalcogenides and dipnictides occupying interstitial sites.[26] Therefore, in Table II we have indicated combinations of metal polyhedral clusters that have the appropriate geometric parameters for stabilizing N_2, B_2, Si_2, Ge_2, As_2, or Te_2 moieties.

Structures Based on Two Trigonal Prisms Sharing a Square Face. The cluster compound $[Co_6Ni_2(CO)_{16}(C_2)]^{2-}$ (1) has a structure based on two trigonal prisms sharing a square face and a total of 116 valence electrons. This conforms to the condensation rules based on two trigonal prisms which have 90 valence electrons (i.e. 90 × 2 − 64 = 116), where 64 is the electron count characteristic of the common square face.[27] This analysis suggests that

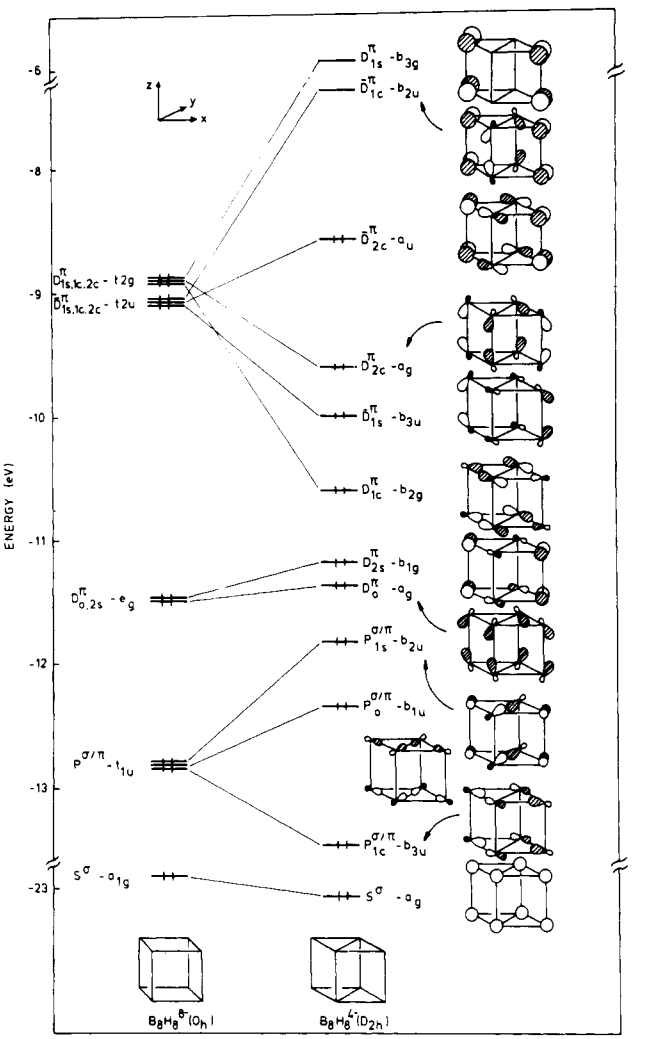

Figure 1. Effect of D_{2h} distortion on the skeletal molecular orbitals of a cube, $B_8H_8^{8-}$.

the D_{2h} skeletal geometry in 1 is characterized by 10 skeletal electron pairs (SEP's). Therefore, the first task of the theoretical analysis is to establish why this electron count occurs and the nature of the interactions between these skeletal molecular orbitals (SMO's) and the molecular orbitals of the C_2 moiety.

In view of the *isolobal* analogy between borane and transition-metal fragments,[28] it is useful to clearly identify the nodal characteristics of these SMO's from model calculations on $B_8H_8^{4-}$. A particularly instructive way of doing this is to derive the D_{2h} $B_8H_8^{4-}$ polyhedron 3 from the cubic $B_8H_8^{8-}$ polyhedron 2 by making two more diagonal bonds across the square faces, as shown below.

(26) See, for example: (a) Aronsson, B. *Borides, Silicides and Phosphides*; Wiley: New York, 1965. (b) Pearson, W. B. *J. Solid State Chem.* **1985**, *56*, 278. For a theoretical study on the $M'M_2X_2$ compounds see: Zheng, C.; Hoffmann, R. *J. Chem. Phys.* **1985**, *89*, 4175.

(27) Mingos, D. M. P. *J. Chem. Soc., Chem. Commun.* **1983**, 706; *Acc. Chem. Res.* **1984**, *17*, 311.

(28) Hoffmann, R. *Angew. Chem., Int. Ed. Engl.* **1982**, *21*, 711.

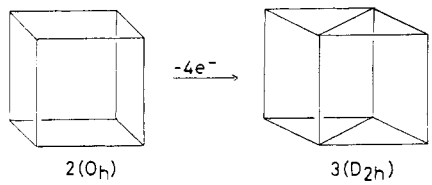

Figure 1 illustrates the effect of introducing such a D_{2h} distortion on the energy levels of the cubic polyhedron **2**. The molecular orbitals of this polyhedron have been analyzed previously[29] within the framework of Stone's tensor surface harmonic theory,[30] and the relevant spherical symmetry labels are given in Figure 1. The radial SMO's $S^{\sigma}(a_{1g})$ and $P^{\sigma}(t_{1u})$ and the tangential $D^{\pi}_{0,2s}(e_g)$ SMO's are only slightly perturbed by the D_{2h} distortion. In contrast the energies of the nonbonding and tangential $D^{\pi}_{1c,1s,2c}(t_{2g})$ and $\bar{D}^{\pi}_{1c,1s,2c}(t_{2u})$ molecular orbitals are strongly influenced by the distortion. The parity relationship connecting these molecular orbitals[29,30] ensures that three of these orbitals, $D^{\pi}_{1c,2c}(b_{2g}, a_g)$ and $\bar{D}^{\pi}_{1s}(b_{3u})$, are stabilized and three orbitals, $D^{\pi}_{1s}(b_{3g})$ and $\bar{D}^{\pi}_{1c,2c}(b_{2u}, a_u)$, are destabilized by approximately equal energies. The occupation of the former three molecular orbitals, together with $S^{\sigma}(a_g)$, $P^{\sigma/\pi}(b_{3u}, b_{1u}, b_{2u})$, and $D^{\pi}_{0,2s}(a_g, b_{1g})$, leads to a total of nine bonding SMO's. In addition, since the $\bar{D}^{\pi}_{2c}(a_u)$ molecular orbital is bonding in the two rhombic planes and π-antibonding across the new diagonal bonds, it is not strongly antibonding and could represent a tenth SMO.

In Figure 2 the molecular orbital interactions between metallic $[Co_8(\mu\text{-}L)_8L_8]^{2-}$ cluster with a C_{2h} symmetry and an interstitial C_2^{2-} moiety located at the centers of the trigonal prisms are illustrated. In the model compound $[Co_8(\mu\text{-}L)_8L_8C_2]^{4-}$ (**4**), the presence of the metal "d band" of molecular orbitals and the interactions with the bridging ligands makes the interpretation of the observed spectrum of molecular orbitals much more complex than that described above for $B_8H_8^{4-}$ (**3**). Nevertheless, in **4** (116 electrons) a set of ten SMO's can be identified that correlate with the ten SMO's of the borane model **3**.

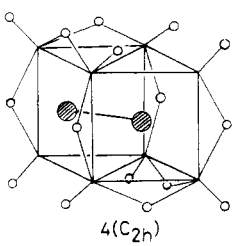

The five most stable molecular orbitals $S^{\sigma}(1a_g)$, $P^{\sigma/\pi}(1b_1, 2b_u, 1a_u)$, and $D^{\pi}_{2c}(2a_g)$ are localized predominantly on the more electronegative C_2 moiety and correlate with the σ_s and σ^*_s, σ_p, and π molecular orbitals of the isolated C_2 molecule. The frontier orbitals are localized to a greater extent on the metal atoms, and the following SMO's can be identified: $D^{\pi}_0(3a_g)$, $D^{\pi}_{2s}(b_g)$, $D^{\pi}_{1c}(4a_g)$, $\bar{D}^{\pi}_{2c}(2a_u)$, and $\bar{D}^{\pi}_{1s}(3b_u)$. The latter mixes with $P^{\sigma/\pi}_0$ and $\bar{D}^{\pi}_{2s}$, which are of same symmetry. The $D^{\pi}_{2s}(b_g)$ and $D^{\pi}_{1c}(a_g)$ metallic molecular orbitals interact significantly with the higher lying C–C π^* molecular orbitals, and a significant amount of electron density is transferred from the cluster molecular orbitals to the antibonding C–C molecular orbitals in this manner.

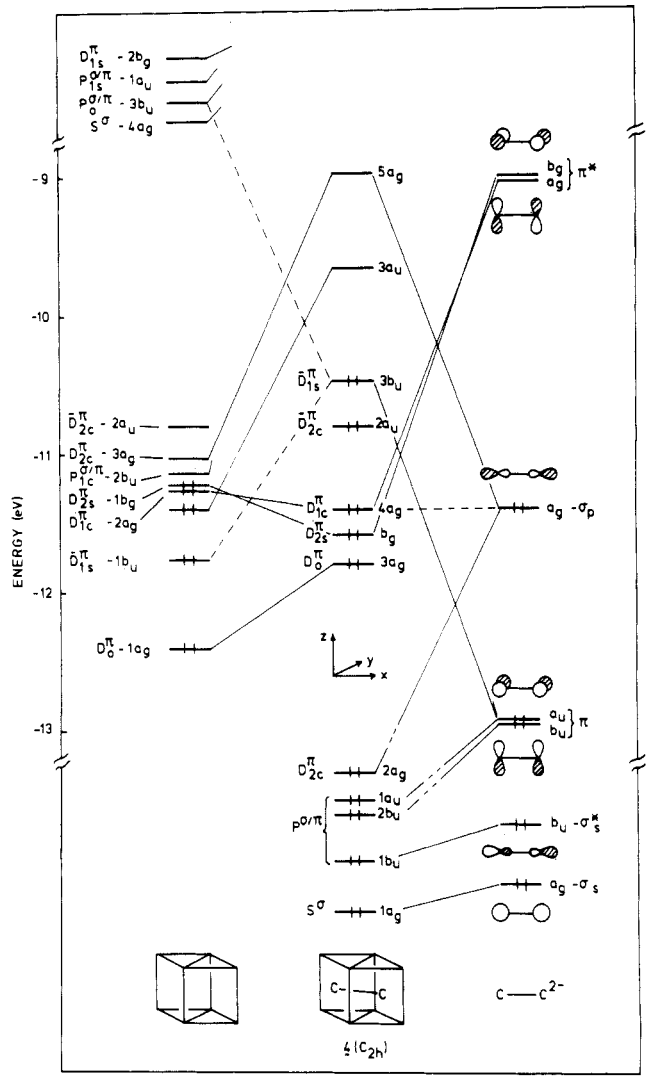

Figure 2. Molecular orbital interaction diagram for $[Co_8(\mu\text{-}L)_8L_8C_2]^{4-}$ (**4**) of C_{2h} symmetry.

The occupation of these 10 skeletal molecular orbitals and the 48 molecular orbitals ($6n$), which represent the cluster d band and the M–L bonding molecular orbitals, leads to a total valence electron count of 116 ($6n + 20$), which is consistent with the condensation rules[27] and the observed electron count in **1**.

The lowest unoccupied molecular orbitals in our model calculations are $\bar{D}^{\pi}_{1c}(3a_u)$ and $D^{\pi}_{2c}(5a_g)$ (the out-of-phase combination), which lie 0.75 and 1.48 eV, respectively, above the ground state. The orbitals that are illustrated in **5** possess approximately 25% C–C character and, more

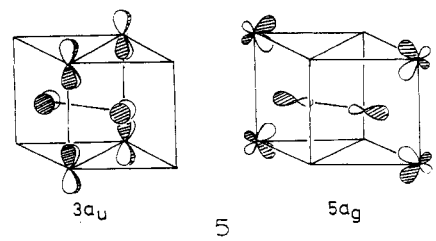

importantly, are C–C bonding and M–C antibonding. Consequently the addition of either two or four electrons to the molecular orbital scheme for **4** would lead to a strengthening of the carbon–carbon bond.

The computed overlap populations for the C–C orbitals in **4** and some related ethanido cluster compounds are summarized in Table III. These results suggest that the

(29) Johnston, R. L.; Mingos, D. M. P. *J. Organomet. Chem.* **1985**, *280*, 407.

(30) (a) Stone, A. J. *Mol. Phys.* **1980**, *41*, 1339. (b) Stone, A. J. *Inorg. Chem.* **1981**, *21*, 563. (c) Stone, A. J.; Alderton, M. J. *Inorg. Chem.* **1982**, *21*, 2297. (d) Stone, A. J. *Polyhedron* **1984**, *3*, 3051.

Table III. C_2 Molecular Interactions

cluster model	polyhedron	VEC[a]	d_{C-C}, Å	C_2 MO occupatn						C–C overlap pop.
				σ^*_p	π^*	σ_p	π	σ^*_s	σ_s	
$[Co_8(\mu\text{-}L)_8L_8C_2]^{4-}$ (4)	bi-trigonal prism (C_{2h})	116	1.47	0.05	0.52 0.56	1.22	1.15 1.46	1.39	1.88	0.90
$[Co_8(\mu\text{-}L)_4L_{12}C_2]^{4-}$ (6)	bi-trigonal prism (D_{2h})	116	1.47	0.05	0.41 0.37	1.16	1.21 1.39	1.43	1.87	0.88
$[Co_8(\mu\text{-}L)_4L_{12}C_2]^{4-}$ (7)	twisted bi-trigonal prism (C_{2v})	116	1.47	0.05	0.40 0.42	1.13	1.21 1.41	1.44	1.87	0.88
$[Co_{10}(\mu\text{-}L)_{10}L_6C_2]^{12-}$ (8)	bicapped bi-trigonal prism (C_{2h})	142	1.47	0.05	0.46 0.53	1.59	1.56 1.51	1.51	1.88	1.08
$[Co_{10}(\mu\text{-}L)_{10}L_6C_2]^{12-}$ (8a)	distorted bicapped bi-trigonal prism (C_{2h})	142	1.47	0.05	0.49 0.48	1.57	1.54 1.57	1.50	1.90	1.11
$[Co_{10}(\mu\text{-}L)_2L_{14}C_2]^{12-}$ (9)	bicapped bi-trigonal prism (C_{2h})	142	1.47	0.04	0.42 0.41	1.59	1.46 1.41	1.46	1.87	1.05
$[Co_{10}(\mu\text{-}L)_{10}L_6C_2]^{12-}$ (10a)	square antiprism–trigonal prism (C_2)	142	1.47	0.06	0.53 0.54	1.50	1.54 1.50	1.50	1.88	1.05
$[Co_{10}(\mu\text{-}L)_{10}L_6C_2]^{12-}$ (10b)	ibid.	142	1.80	0.16	0.69 0.72	1.51	1.47 1.41	1.47	1.79	0.58
$[Co_{10}(\mu\text{-}L)_{10}L_6C_2]^{12-}$ (10c)	ibid.	142	2.10	0.33	0.80 0.84	1.49	1.33 1.45	1.48	1.70	0.31
$[Co_{10}(\mu_3\text{-}L)_8L_{10}C_2]^{8-}$ (14)	bicapped square, antiprism (D_{4d})	142	1.47	0.04	0.52	1.05	1.46	1.25	1.89	0.98
$[Co_{10}(\mu_3\text{-}L)_8L_{10}C_2]^{8-}$	ibid.	142	2.14	0.30	0.72	1.09	1.27	1.30	1.66	0.25
C_2H_6 ethane		14	1.54	0.03	0.87	1.59	1.03	1.03	1.67	0.65
C_2H_2 acetylene		10	1.20	0.00	0.00	1.12	2.00	1.20	1.92	1.93
C^{2-}		10	1.20	0.00	0.00	2.00	2.00	2.00	2.00	1.89

[a] Valence electron count.

bonding between the C_2 moiety and the cluster is rather covalent in nature and synergic. In **4** the C_2 π molecular orbitals donate 1.39 electrons to the cluster, and the C_2 π^* orbitals accept 1.08 electrons from the cluster. These synergic interactions are reflected in the computed C–C overlap population of 0.90, which corresponds approximately to a C–C bond order of 1.3. The observed C–C bond length of 1.494 Å in **1** is consistent with a bond order of between 1.0 and 1.5.

In the calculations on the model compound **6** that has the same skeletal geometry as **4** but a different arrangement of ligands that reflects the D_{2h} symmetry of the skeleton, the computed overlap population is also ca. 0.90, although this is achieved by less donation from C_2 to the skeleton and more back donation. The precise ordering of the SMO's also differs from **4** but does not appear to greatly affect the C–C bonding.

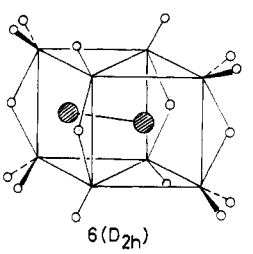

6(D_{2h})

In **7**, which currently does not have a characterized analogue, the two trigonal prisms have been rotated relative to each other leading to a cluster of C_{2v} symmetry. The computed C–C overlap population and the total one electron energies for **4** and **7** are very similar, suggesting that the metal skeletons in these clusters may undergo facile polytopal rearrangements relative to the C_2 core.

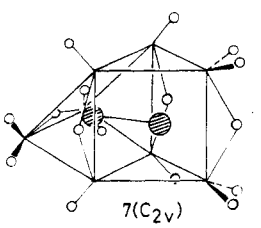

7(C_{2v})

We have also completed molecular orbital calculations on **8** and **9** that have skeletal geometries based on two capped trigonal prisms sharing a common square face.

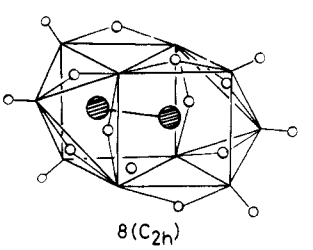

8(C_{2h})

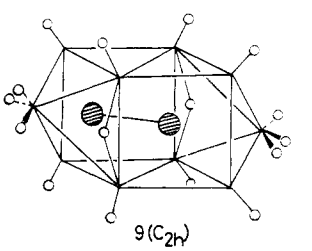

9(C_{2h})

From Table III it is apparent that the computed C–C overlap populations in these clusters are significantly larger, i.e. 1.05–1.08. This difference can be traced primarily to a greater population of π_y and σ_p and is associated with the stabilization and population of the $\bar{D}^{\pi}_{1c}(3a_u)$ and $D^{\pi}_{2c}(5a_g)$ orbitals illustrated in **5**. The cluster compound $[Ni_{10}(CO)_{16}(C_2)]^{2-}$ has this skeletal geometry and the ligand arrangement illustrated in **8**. The observed C–C bond length of 1.405 Å is significantly shorter than that noted above for **1** (1.494 Å) and is consistent with the larger computed overlap population. $[Ni_{10}(CO)_{16}(C_2)]^{2-}$ has a total of 142 valence electrons that is consistent with the presence of 11 SEP's. Strict application of the capping principle[31] suggests that **8** and **9** should have the same number of skeletal bonding molecular orbitals as the parent uncapped cluster **4**, i.e. 10. We have described in some detail elsewhere how the introduction of capping atoms can result in the stabilization of one SMO, if they define a torus, or three SMO's, if they define a complete polyhedron.[29,32] In **8** and **9** the occurrence of one additional molecular orbital arises from the stabilization of $\bar{D}^{\pi}_{1c}(3a_u)$ and $D^{\pi}_{2c}(5a_g)$ and the destabilization of one of the metal skeletal molecular orbitals. When the spectrum of molecular orbitals for **8** is filled with 142 electrons, a stable,

(31) Mingos, D. M. P.; Forsyth, M. I. *J. Chem. Soc., Dalton Trans.* **1977**, 610.
(32) Johnston, R. L.; Mingos, D. M. P. *J. Chem. Soc., Dalton Trans.* **1987**, 1445.

closed-shell structure with a substantial HOMO–LUMO energy gap of 2.20 eV is calculated. Calculations on $[B_{10}H_{10}]^{2-}$ with the skeletal geometry illustrated in **8** have shown that it also has 11 skeletal bonding molecular orbitals.

The crystallographic determination on $[Ni_{10}(CO)_{16}(C_2)]^{2-}$ has demonstrated that each carbon atom is effectively bonded to seven nickel atoms. This is achieved by a skeletal compression involving the capping atoms. We have modeled this distortion in the calculations, and the results are summarized in Table III as entry **8a**. The computed C–C overlap population increases to 1.11. The bonding of the C_2 dimer is quite similar to that of the undistorted model **8**.

The cluster compounds $[Co_3Ni_7(CO)_{15}(C_2)]^{3-}$ and $[Co_3Ni_7(CO)_{16}(C_2)]^{2-}$ have related geometries but are severely distorted and have low symmetries. Consequently we have not attempted to model these compounds in our calculations. These compounds are of some interest, nonetheless, because they have only 138 and 139 valence electrons, respectively.[10,11]

Structures Based on a Trigonal Prism and a Square Antiprism Sharing a Square Face. Although the centroids of the trigonal prism and the square antiprism are separated by 1.80 Å (see Table II), the carbon–carbon distance can vary from 1.40 to 2.20 Å and still maintain reasonable metal–carbon bond lengths. Three representative calculations on $[Co_{10}(\mu\text{-L})_{10}L_6C_2]^{12-}$ (**10**) with

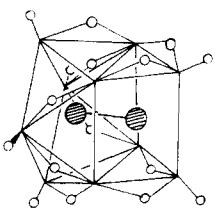

10(C_2)

C–C separations equal to 1.47, 1.80, and 2.10 Å are summarized in Table III (**10a**, **10b**, and **10c** respectively). Although the optimization of atomic distances is unsatisfactory within the extended Hückel approximation, it is remarkable how soft the potential energy surface is for elongation of the C–C bond (only 1.10 eV). A significant HOMO–LUMO gap is maintained for this distortion coordinate (1.92–1.17 eV), and the absence of level crossings makes the C–C scission a symmetry-allowed process. Even at a C–C separation of 2.10 Å although the C_2 π^* molecular orbitals are only weakly antibonding, they lie above the filled metal cluster orbitals. Along the distortion coordinate the loss in bonding of the C–C bond is compensated for by stronger metal–carbon bonding interactions.

Although structure **10** has not been observed, the closely related capped derivatives $[Co_{11}(CO)_{22}(C_2)]^{3-}$ (**11**) and $Rh_{12}(CO)_{25}(C_2)$ (**12**) have been studied.[14,18] In the monocapped derivative **11**, the C–C distances lies between 1.62 and 1.66 Å, whereas in the bicapped derivative **12**, the C–C

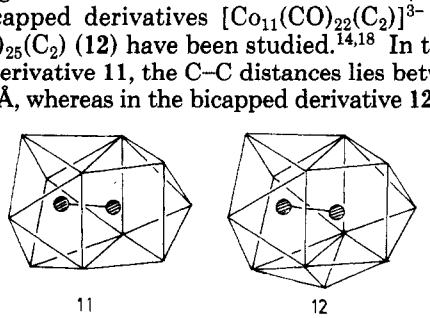

11 12

distance is only 1.48 Å. These results are consistent with the occurrence of a soft potential energy surface. Chemical degradation studies suggesting the formation of C_2 hydrocarbons from polycarbido clusters are also consistent with the facile transformation of separated carbido atoms into C_2 units.[7]

The calculations on model **10a** suggest that a reasonably large HOMO–LUMO separation of 1.92 eV is observed for a total of 142 valence electrons, i.e. 11 SEP's. Interestingly the characterized capped derivatives **11** and **12** both have a total of 11 skeletal bonding electron pairs.

The square antiprism–trigonal prismatic condensed pair **9** is characterized by the same closed-shell requirements as the capped trigonal prism condensed pair **8**, i.e. 142 valence electrons.

Structures Based on Two Square Antiprisms Sharing a Square Face. For a metal–metal distance of 2.54 Å the centroids of the two associated square antiprisms are separated by 2.136 Å. Therefore our initial model calculations on $[Co_{12}(\mu\text{-L})_8L_{16}C_2]^{2-}$ (**13**) had the

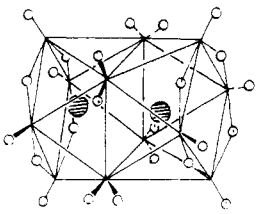

13(C_{2v})

carbon atoms placed at these locations. At this length the C–C π^* orbital is low-lying and a substantial amount of electron density is transferred from the metal to these orbitals.

Variation of the C–C distance from 1.40 to 2.80 Å has demonstrated that at the latter distance the compound is more stable by at least 2.0 eV. Therefore one anticipates that this skeletal framework is geometrically and electronically unfavorable for stabilizing a bonded C_2 unit. $[Rh_{12}(CO)_{23}(C_2)]^{4-}$ and $[Rh_{12}(CO)_{24}(C_2)]^{2-}$ have skeletal geometries that can be related to a pair of square antiprisms sharing a face and have a total of 166 valence electrons.[16,17] The C–C distances in these clusters are 3.37 and 3.30 Å, respectively. Besides showing the anticipated long C–C distance the central square of metal atoms in the idealized structure is distorted to form a rhombus with a short diagonal rhodium–rhodium distance of ca. 2.75 Å. This distortion improves the strength of metal–carbon bonding at the individual carbon atoms.

Bicapped Square Antiprism. The bicapped square antiprism represents an alternative skeletal geometry that is also characterized by a total of 142 valence electrons. Although the carbido clusters $[Ni_{10}(CO)_{18}C]^{2-}$ (bicapped square antiprism), $[Ni_9(CO)_{17}C]^{2-}$ (capped square-antiprism), and $[Ni_8(CO)_{16}C]^{2-}$ (square antiprism) have been characterized,[33] geometric calculations suggest that the central cavity in such clusters is rather too large and in the bicapped square antiprism could accommodate a C_2 moiety with a C–C bond length of 1.47 Å and metal–carbon distances of 1.82 (with M_{basal}) and 2.13 Å (with M_{apical}). Therefore, we have completed calculations on the model compound $[Co_{10}(\mu_3\text{-L})_8L_{10}C_2]^{8-}$ (**14**) with an idealized D_{4d} geometry. The ligand geometry is similar to that reported for $[Ni_9(CO)_{17}C]^{2-}$ which has a capped square-antiprismatic skeletal geometry.[33]

The molecular orbital interaction diagram for **14** that is illustrated in Figure 3 suggests that such a ethanido cluster would have a closed-shell electronic configuration for 142 electrons. The 11 skeletal bonding molecular or-

(33) Ceriotti, A.; Longoni, G.; Manassero, M.; Perego, M.; Sansoni, M. *Inorg. Chem.* **1985**, *24*, 117.

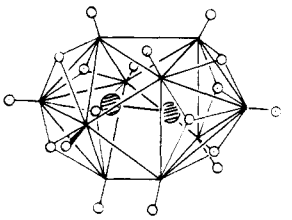

14(D_{4d})

bitals may be assigned the following tensor surface harmonic theory labels $S^{\sigma}(1a_1)$, $P^{\sigma/\pi}(1b_2, 1e_1)$, $D^{\pi}_0(2a_1)$, $D^{\pi}_{1s,1c}(1e_3)$, $F^{\pi}_{1s,1c}(2e_1)$, and $D^{\pi}_{2c,2s}(e_2)$ and correspond to the same SMO's as those associated with the *closo*-borane anion $[B_{10}H_{10}]^{2-}$.[34] The HOMO's are a degenerate pair of e_2 molecular orbitals that are localized exclusively on the metal skeleton. The LUMO $3a_1$ results from an out-of-phase overlap between $D^{\pi}_0(a_1)$ and the C_2 $\sigma_p(a_1)$ molecular orbital and is localized predominantly on the carbon atoms. It is apparent from Table III that the C_2 unit enters into a similar synergic bonding interactions with the metal cage as those reported previously for **8** and **10a**.

When the C–C bond length is increased in **14** from 1.47 to 2.13 Å, the total energy increases considerably (2.35 eV). This behavior is quite different from that noted earlier for **10** and **13**, where a rather soft potential energy surface was noted for the C–C lengthening distortion (actually a slight stabilization).

The different characteristics of the potential energy surfaces can be related to the nodal characteristics of the metal skeletal molecular orbitals in **10**, **13**, and **14**. In **10** and **13** the primary bonding interactions result from the overlap between C_2 π and the higher lying metal $P^{\sigma/\pi}$ orbitals (see **15**). For these three layer structures the overlap integral between these orbitals is insensitive to the C–C distance because the loss of overlap with the central layer of metal atoms is compensated for by an increase in overlap with the outer layers of metal atoms (see **15b**). The nodal characteristics of the metal D^{π} orbitals do not lead to strong overlap with the C_2 π orbitals.

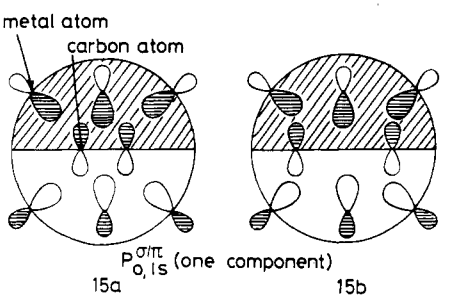

For **14** the predominant overlap for C_2 π occurs with the $P^{\sigma/\pi}$ orbitals at short internuclear distances (see **16a**). However, there is also a significant interaction with the filled metal $F^{\pi}_{1s,1c}$ skeletal orbitals shown in **16b**. As the C–C bond is lengthened, the former interaction decreases and the latter increases (see **16**) and as a result the four-electron destabilizing interaction between C_2 π and $F^{\pi}_{1s,1c}$ assumes a greater importance. It is this destabilizing effect that resists the lengthening of the C–C bond.

These results suggest that if a C_2 moiety is incorporated within a bicapped square-antiprismatic cluster, it will have a short C–C bond length. The C–C distances in a series of such compounds will not vary over a wide range. The

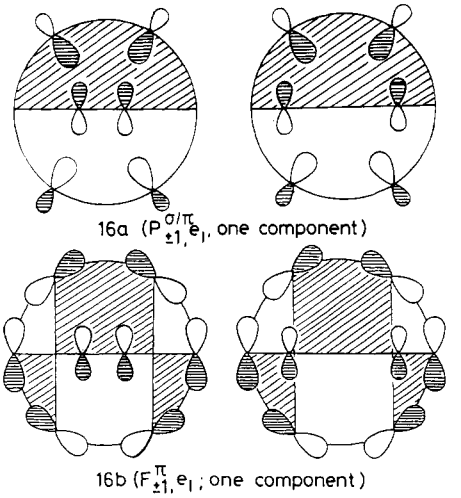

major bonding interactions result from the overlap of the carbon 2s and 2p orbitals with the equatorial metal atoms rather than the apical ones. For a C–C bond length of 1.47 Å the computed overlap populations are 0.35 for C–$M_{equatorial}$ and 0.09 for C–M_{apical}. Elongation of the C–C bond to 2.54 Å improves both overlap populations to 0.42 and 0.21, respectively, but there is a corresponding decrease in the C–C overlap population from 0.98 to 0.25.

It is remarkable that a staggered condensation of two well-known square-pyramidal molecules $Fe_5(CO)_{15}C$[35] would lead to such a geometry, **14**. Note finally that the arguments described above are also valid for a bicapped cubic polyhedron.

Conclusions

The molecular orbital studies described above have indicated that the interstitial C_2 fragment enters into a synergic bonding interaction with the skeletal molecular orbitals of the metal cage. Electron donation occurs primarily from the C_2 σ_p and π bonding molecular orbitals to the cage $P^{\sigma/\pi}$ and D^{π}_{2c} orbitals and is supplemented by back donation from filled cage $D^{\pi}_{1c,2s}$ orbitals to the C_2 π^* orbitals. The net result is a C–C formal bond order between 1.0 and 1.5 and an approximately electroneutral C_2 moiety as observed in the ethane molecule (see Table III). While the Chatt–Dewar–Ducanson bonding model is well-established for acetylene complexes[36] and acetylene chemisorbed on metal surfaces,[37] the importance of synergic interactions for polyatomic moieties in carbonyl cluster cage compounds has not been stressed previously.

The potential energy surface for C–C bond lengthening in the dicarbido clusters is relatively soft and the observed C–C bond length depends critically on the geometric factors imposed by the metal cage. For two capped or noncapped trigonal prisms sharing a square face the distance separating the two interstitial cavities is approximately equal to a single C–C bond length and the location of carbon atoms in these cavities leads to satisfactory C–C bond lengths. In contrast for condensed polyhedra generated from the sharing of a square face of a square antiprism the intercentroid distances are much longer, and longer C–C distances are predicted for dicarbido com-

(34) (a) Johnston, R. L.; Mingos, D. M. P. *J. Organomet. Chem.* **1985**, *280*, 419. (b) Johnston, R. L.; Mingos, D. M. P. *J. Chem. Soc., Dalton Trans.* **1987**, 647.

(35) Braye, E. H.; Dahl, L. F.; Hübel, W.; Wampler, D. L. *J. Am. Chem. Soc.* **1962**, *84*, 4633.

(36) See, for example: (a) Mingos, D. M. P. In *Comprehensive Organometallic Chemistry*; Wilkinson, G., Stone, F. G. A., Abel, E. W., Eds.; Pergamon: Oxford, 1981; Vol. 3, p 1. (b) Hoffman, D. M.; Hoffmann, R.; Fisel, C. R. *J. Am. Chem. Soc.* **1982**, *104*, 3858. (c) Schilling, B. E. R.; Hoffmann, R. *J. Am. Chem. Soc.* **1979**, *101*, 3456.

(37) Silvestre, J.; Hoffmann, R. *Langmuir* **1985**, *1*, 621.

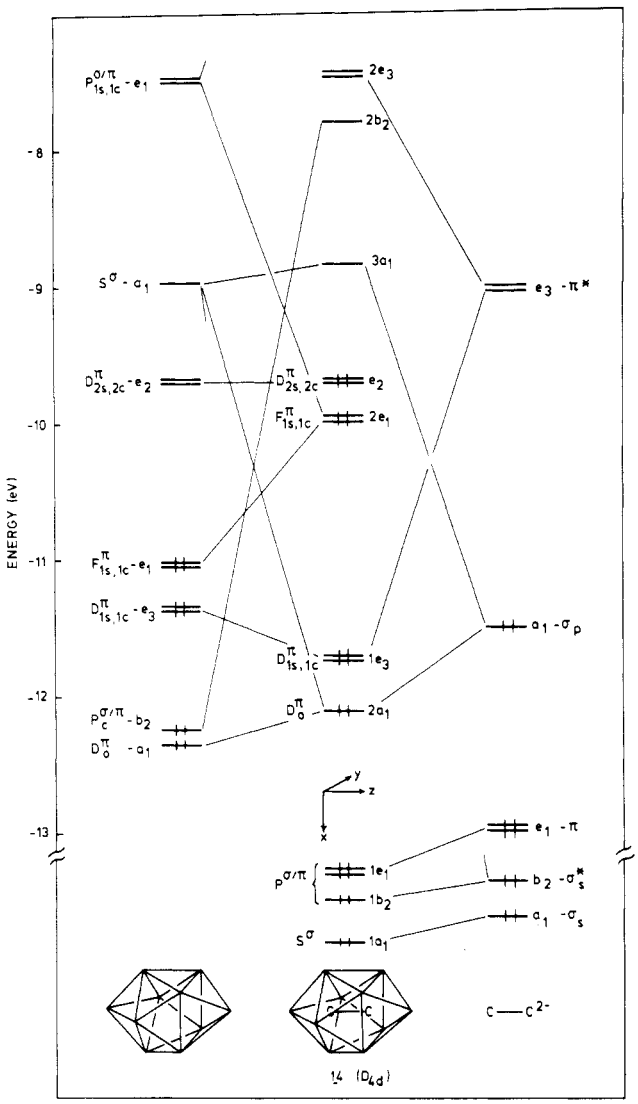

Figure 3. Molecular orbital interaction diagram for $[Co_{10}[\mu_3\text{-}L)_8L_{10}C_2]^{8-}$ (**14**) of D_{4d} symmetry.

pounds based on these polyhedra.

The geometric advantages associated with trigonal prisms sharing square faces appear to be carried over to three-dimensional infinite solids. The AlB_2 structures that is adopted by many transition-metal borides and is illustrated in **17** has an infinite array of trigonal prisms sharing

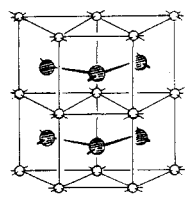

17

square faces and linked boron atoms.[38] The absence of a corresponding three-dimensional carbido structure is probably associated with the relative energies of the Fermi level and the π^* orbitals of the main-group atom. In addition the B–B distance in the sheet is much longer (0.3 Å) than that in graphite.

Calculations on isostructural dicarbido and dinitrido cluster compounds have indicated a much weaker nitrogen–nitrogen interaction in the latter. The greater stability of the N–N π^* molecular orbitals leads to substantially more electron transfer from filled metal levels to these N–N π^* orbitals.

The potential energy surfaces for polytopal rearrangements of the metal cage relative to a fixed C–C moiety are likely to be soft, and the observed cage geometry could be influenced significantly by the number of carbonyl ligands coordinated to the metal cluster.

The great majority of the characterized dicarbido cluster compounds are associated with a total valence electron count of $12n_s + 22$ electrons. The molecular orbital calculations that we have completed on a range of cage geometries suggest that five of the molecular orbitals are localized predominantly on the C–C unit and in tensor surface harmonic terms correspond to S^{σ}, 3 $P^{\sigma/\pi}$, and D^{π}_{2c}. In addition the structures where the C–C vector lies within three layers of metal atoms have an additional set of six molecular orbitals localized mainly on the metal and have nodal characteristics associated with 3 D^{π} and 3 $\bar{D}^{\pi}$ surface harmonic functions.

Appendix

The calculations were performed within the extended Hüchel method.[39] The atomic parameters utilized for Co metal were taken from literature.[40] Computer size limitations prevented us from introducing CO ligands that were modeled by H^- in our calculations. The geometry models were derived from X-ray crystallographic data. The following bond distances (Å) were used: B–B = 1.70, B–H = 1.20, Co–Co = 2.54, Co–H = 1.70. When not specified, a C–C distance of 1.47 Å was assumed.

Acknowledgment. The SERC is thanked for financial support and Dr. Roy L. Johnston and Lin Zhen Yang for helpful comments. J.-F.H.'s stay at Oxford was made possible by a grant from an Exchange Program between the Royal Society and the CNRS.

Registry No. **4** (M = Co, L = H), 110825-21-3; **6** (M = Co, L = H), 110825-22-4; **7** (M = Co, L = H), 110825-20-2; **8** (M = Ni, L = CO), 97759-11-0; **8** (M = Co, L = H), 110848-56-1; **9** (M = Co, L = H), 110795-69-2; **10** (M = Co, L = H), 110873-95-5; **11**, 81220-79-3; **12**, 67801-78-9; **14** (M = Co, L = H), 110900-31-7; $[Rh_{12}(CO)_{23}(C_2)]^{4-}$, 88121-70-4; $[Rh_{12}(CO)_{24}(C_2)]^{2-}$, 79176-35-5.

(38) For a theoretical study see: Burdett, J. K.; Canadell, E.; Miller, G. J. *J. Am. Chem. Soc.* **1986**, *108*, 6561.

(39) (a) Hoffmann, R. *J. Chem. Phys.* **1963**, *39*, 1397. (b) Hoffmann, R.; Lipscomb, W. N. *Ibid.* **1962**, *36*, 2179, 3189; **1962**, *37*, 2872.

(40) Summerville, R. H.; Hoffmann, R. *J. Am. Chem. Soc.* **1976**, *98*, 7240.